Acoustic Loss Tomography: Identification of phonon attenuation in high-Q mechanical resonators

A. Roche,[1] A. Markowitz,[2] and R. X Adhikari[2]
[1)] *Physics Department, University of Washington.*
[2)] *LIGO, California Institute of Technology*

(Dated: 13 October 2019)

Thermal noise is important in areas such as gravitation wave detection and mechanical resonators since they rely upon extremely precise measurements. When measurements become extremely precise, quantum observables are being measured. These quantum observables can be measured in an isolated system, but in an environment with uncontrolled degrees of freedom, classical noise becomes a limiting factor of precision. This precision is limited by thermal fluctuations, prompting our focus on improving the quality factor of mechanical oscillators in the Gentle Nodal Suspension system. In order to minimize energy loss, we must better understand how competing frequencies depend on different mechanical losses. The resonator oscillation frequency can couple with different sources throughout the system. We will work to isolate these mechanical losses in the system, model and experimentally verify their frequency dependence, in order to lower this loss in the suspension system.

I. INTRODUCTION

This experiment is a cryogenic version of the Gentle Nodal Suspension system for measuring Q-factors of mechanical resonators. In order to increase the Q-factor of this system, we will focus initially and substantially on the intrinsic loss in the silicon near the zero crossing point of its thermal expansion coefficient. At this zero point, some dominant losses and noise contributions drop to zero. A better understanding of the losses in the silicon could prove invaluable, as this thin film is used to coat highly reflective surfaces in the LIGO cryogenics. These silicon coatings store a small fraction of the energy in the acoustic modes, so the additional mechanical losses must be even smaller. To accurately measure the silicon coating losses, other losses must be subdominant.

We will calculate a loss budget for the silicon wafers, looking at surface and bulk losses and what happens at the contact point of the suspension system. The quality of gravitational wave detection in the next generation of LIGO (LIGO Voyager) facilities are limited by thermally induced vibrations in the mirrors which becomes noise in the interferometers. In LIGO Voyager, quantum noise will be brought down, which will cause thermal noise to become the limiting factor in measurement accuracy. In order to reduce thermal noise, low temperature mirrors made of high purity single-crystalline silicon will be used. One further complication comes from the potential of mechanical vibrations of the mirror and any other surfaces at these cryogenic temperatures. Such vibrations can cause a noise inducing phase shift on the light within the interferometer. Thermal noise appears in Brownian motion. Direct displacement noise in the form of Brownian noise is one form of thermal noise. Others include thermally induced shifts in the refractive index of the material and thermally induced strain causing the optics to change shapes. Brownian noise is the main focus for highly reflective coatings.

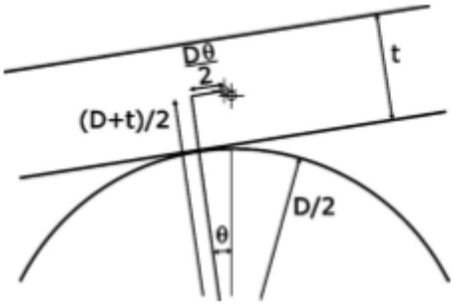

FIG. 1. Diagram of Gentle Nodal Suspension system: the sapphire lens touches the silicon disk at a single node.

To tackle this problem, thin film silicon coatings are used. Silicon is a clear choice at cryogenic temperatures its mechanical loss decreases with temperature, which is not seen in fused amorphous silica. At 124 K silicon's thermal expansion coefficient crosses zero and at this zero crossing, thermoelastic component of the thermal noise is eliminated. Also, silicon has very high thermal conductivity. This allows for higher laser powers since the thermal lensing of the mirror is reduced, and it is easier to remove any absorbed heat.

II. LOSS TOMOGRAPHY

Loss tomography combines experimental measurements and finite element modeling results to solve for the contributions from loss sources. For a simple example, consider the experimental measurement of two eigenmodes of the silicon wafer. Given two measurements, we can determine two parameters without having the calculation underparameterized[?].

$$\begin{aligned} \phi_1 &= \alpha_1 \phi_{1,bulk} + \beta_1 \phi_{1,coat} \\ \phi_2 &= \alpha_2 \phi_{2,bulk} + \beta_2 \phi_{2,coat} \end{aligned} \tag{1}$$

Here, ϕ_1 and ϕ_2 are the measured loss angles calculated from the Q factor, $\phi = 1/Q$,of the associated eigenmode measured on the nodal suspension system. Using COMSOL Multiphysics Modeling, the strain energy loss due to the bulk versus coating can be calculated, allowing the weighting coefficients

α and β to be calculated. With the weighting coefficients determined through FEA (strain energy ratio (SER) calculations), the loss contributions can be easily calculated though matrix inversion of the coefficient matrix.

$$\begin{pmatrix} SER_{bulk,1} & SER_{surface,1} \\ SER_{bulk,2} & SER_{surface,2} \end{pmatrix}^{-1} \begin{pmatrix} \phi_1 \\ \phi_2 \end{pmatrix} = \begin{pmatrix} \phi_{unknown,1} \\ \phi_{unknown,2} \end{pmatrix} \quad (2)$$

This matrix inversion can be expanded to find more loss sources through more Q factor measurements. With information about the loss sources and their impact in different modes, the optimal mode for varying conditions can be found. For example, some modes will have different responses in bulk versus coating loss and this can be used to excite the modes with less loss.

A. Q factor: Fitting and Optimization

In order to calculate the loss angle required for loss tomography, the experimental data must be fit with a very low uncertainty. There are two methods used to find the Q factor of the silicon disk. The first, using a single butter worth bandpass filter to excite different modes. Once a mode is excited the excitation can be turned off, and the data from a quadrant photo diode (QPD) can be analyzed to find the power spectrum density (PSD) and decay of the mode.

1. Heterodyning

Heterodyning is a signal processing technique which creates new frequencies by mixing two frequencies. For calculating Q factors, two sine signals at frequencies f_{ij} and $f_{ij}+C$ are mixed, creating two new signals. Here the constant C represents some offset value, which can be optimized for the best fit. One signal is the sum of the two frequencies, and the other is the difference. Using a low pass filter, the difference signal is kept by low passing at $(1.5*C)/Nyquist\,frequency$. This creates a signal of the beats created by the two frequencies, and the decreasing amplitude can be seen over the course of the ring down. The decreasing amplitude of the remaining sine wave it fit using the function,

$$f(t) = A\sin(\omega t+\phi)e^{t/\tau}+C \quad (3)$$

The Q factor is directly related to τ by

$$Q = \pi\tau f_{ij} \quad (4)$$

The optimal mixing signal frequency and time segment for fitting was determined, resulting in the lowest measure of variance. Variance was taken as a weighted trace of the covariance matrix, where fit values τ and ω were weighted by a factor of 10^8, in order to properly see their effects under different fitting parameters. Variance was minimized at a mixing offset of approximately 0.745 using a range beginning at the second largest crest of the decaying cosine wave and ending at the last recorded data point. The range of the fit was

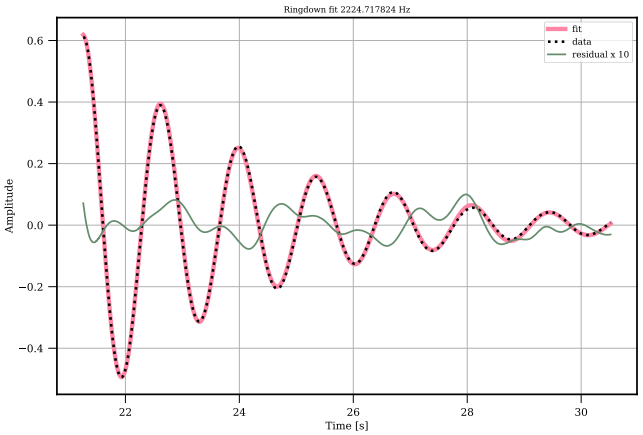

FIG. 2. Fitted exponential ring down decay at 2224.72 Hz including plot of the difference between data and fit, variance = $2.23*10^{-1}$; mixing offset = 0.745.

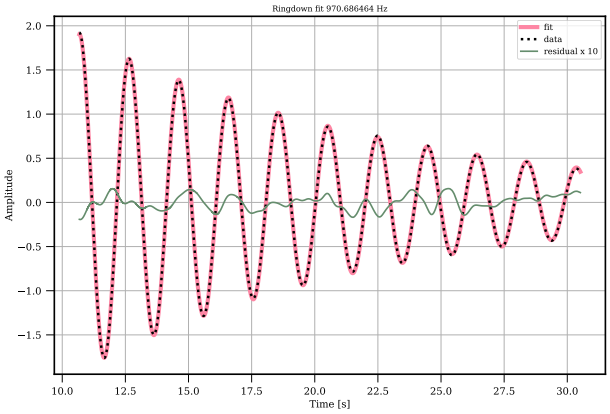

FIG. 3. Fitted exponential ring down decay at 970.69 Hz, variance = $4.94*10^{-}8$; mixing offset = 0.5 Hz.

standardized by adding 10^4*C to the starting index of the fit. This combination of mixing frequency and fitting range resulted in a variance of $2.23*10^{-1}$. The weighted variance was evaluated to be $3.99*10^{-1}$. This fitting method was then used to optimize the fits of eigenmode excited at 970.69 Hz. At 970.69 Hz, the heavily weighted variance was $1.71*10^{-}3$. The fit variance from a 0.5 Hz offset in the mixing frequency resulted in minimum value at 4.9410^{-8}. From the results of the exponential ring down fit, τ can be calculated for each mode and the room temperature Q factor is calculated using Eq.4 as shown in Table I.

TABLE I. Time constants and Q factors of disk 7 at room temperature

Frequency(Hz)	Tau	Q factor	$\sigma^2(w)$	$\sigma^2(fit)$
$9.71*10^2$	12.52	$3.82*10^4$	$1.71*10^{-3}$	$4.94*10^{-8}$
$2.22*10^3$	3.02	$2.11*10^4$	$3.99*10^{-1}$	$2.23*10^{-1}$

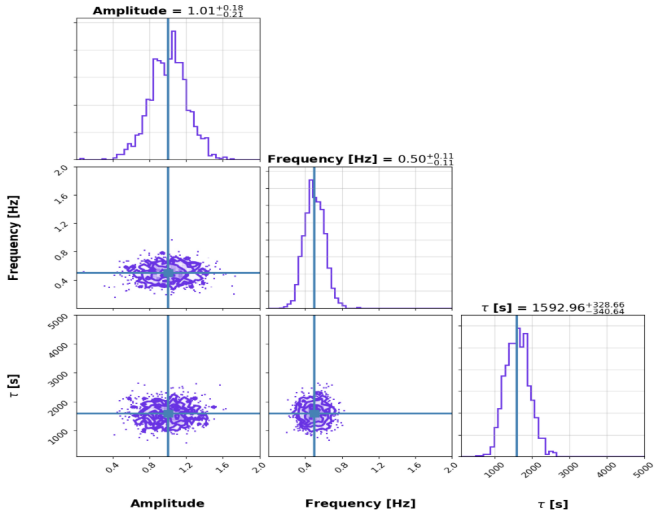

FIG. 4. Corner plot of MCMC model of an exponentially decaying sine wave. Parameter space of τ, ω, and amplitude.

2. *Monte Carlo Markov Chain fittings*

τ values, mode frequency, and amplitude can also be solved using a Monte Carlo Markov Chain (MCMC) simulation. This method is used to approximate the distribution of signal's parameter space. MCMC fit's the parameters through random sampling of a probabilistic space. This method was run on an exponentially decaying sine wave, creating a corner plot of the parameter distributions. This method replaces the fitting method used the the previous section. By fitting the simple ring down data parameter space (Figure 4), it is believed that this code can be adjusted to fit a large parameter space for the final loss tomography calculations.

3. *Cold Mode Ringer Results*

Using an amplitude-locked loop we can calculate how much energy a mode is dissipating by measuring how much energy is put into the mode at equilibrium. This allows continuous measurement of Q-factors to be taken while also recording the amplitude of the excited mode. Using this system, the Q factor and time constant, τ, can be found through fitting the decaying amplitude of the excitation once the power driving the loop is shut off. Additionally, this loop allows for multiple modes to be excited and observed simultaneously. In a cold environment, two modes were excited through the amplitude locked looped, and the ring down in amplitude was fit using an exponential decay function,

$$f(t) = Ae^{t/\tau} + C \tag{5}$$

Once the Q value of a ring down is measured, using the ϕ, C, and H outputs in the loop, the lock-in process in calibrated to match the calculated Q factor. After one calibration, the results of the remainder of the experiment are also calibrated until the excitation is stopped and the disk is removed

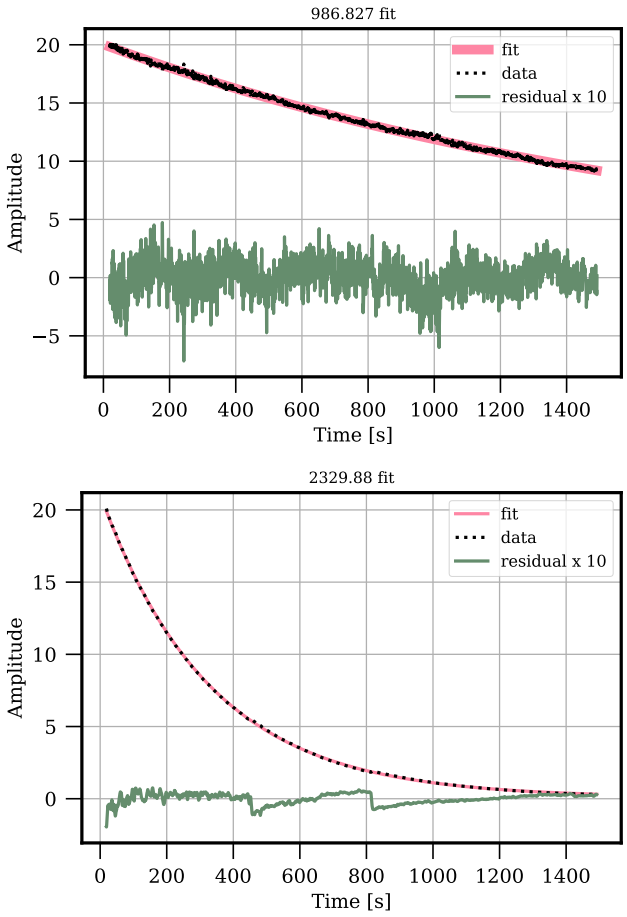

FIG. 5. Fitted exponential ring down decay of amplitude at 986.83 and 2329.8 Hz, cold

TABLE II. Time constants and Q factors of disk 6 - cold

Frequency (Hz)	Tau	Q factor	σ^2
986.83	1876.39	5817208.46	$2.51*10^{-3}$
2329.88	330.345	2417971.34	$1.47*10^{-6}$

or changed.

This system will allow many Q factors and sub sequential loss angles to be calculated. With more of these calculations, more loss contributions can be modelled and solved for using the matrix inversion technique, so far only applied to pairs of losses. This technique provides better fitting results with lower variance and allows for continuous measurements of Q and will be used predominately moving forward in loss tomography studies.

B. Finite Element Analysis

The silicon wafers[5], used in the nodal suspension system are modelled using COMSOL Multiphysics in order to calculate the loss coefficients. Values calculated for elastic strain

energy loss in the bulk of the wafer versus the surface are the coefficients of the losses in the tomography model(1).

The modelled eigenmodes begin at the f_{20} mode, since the first drum mode is not excited in the physical wafers. The first mode was calculated to be 400.57 Hz, and then in increasing frequencies modes are seen at 412.36, 671.66, 929.42, 953.09 Hz and upwards. Using room temperature measurements of eigenfrequencies in the nodal suspension system, parameters used in the model were systematically varied to represent the experimental frequency results. The most accurate model of the wafers was created by looping over the wafer's thickness, radius, and flat sides according to the standard deviation provider by the supplier. Using Fminsearch(MATLAB) on the thickness of the disk resulted in a calculated 314.88 um thickness which corresponds to an eigenfrequency at room temperature of 970.67 Hz. This is in comparison to the measured room temperature frequency of 970.6585 for disk 7. A second COMSOL model with $5\mu m$ thick coating had a minimum variance between the experimental data with a thickness of 309.88 um resulting in a frequency of 970.66 in reference to experimental 970.6585 Hz. These numbers correspond well to what is expected. The coated COMSOL model was run with the coating material set to silicon. Therefore, one would expect the thickness of the disk to be $5\mu m$ less than the thickness of the disk with out a coating, in order to get the same resulting frequency. By looping over the wafer's thickness, radius, and flat sides according to the standard deviation provider by the supplier - the COMSOL model frequency of the 970.6865 Hz mode reached the value 970.66 Hz, a variance of $7.02 * 10^{-4}$.

With the size parameters modified to represent physical conditions, the material properties were then analyzed. The Young's modulus and Poisson's ratio of silicon were examined with slight deviation around the 'Materials and Constants' values found in LIGO documentation. With these modifications, the difference between modelled and experimental eigenmodes was minimized following $|f_0 - f_{COMSOL}|^2$ to a value of (fill in).

1. Bulk and Coating/Surface Loss

(Add background/info about wafer coating types and uses) The first loss tomography study had been conducted on loss contributions from the bulk of the wafer in comparison to a $5\mu m$ coating on the top of the disk. The strain energy ratio (SER) was computed for the bulk and coating volumes of the disk, as well as the total geometry. A coating was created as a thin extrusion from the plane of the disk, and meshed accordingly. In the current model the coating is set to made of silicon, so the different in strain is very minimal. Once the losses of the silicon bulk are as low as possible, the losses of various thin film coatings can be measured with higher confidence that loss from the silicon is significantly effecting the thin film measurements. In the example of the silicon coating it is still clear that the SER differs between modes. The difference between strain in the bulk vs. coat are the two parameters investigate in Figure 7, made evident by the inverse relation between the graphs. Certain modes excite greater displacement in the edges and surface of the disk than other, so understanding how bulk and surface losses contribute to the total loss angle will allow for modes with lower loss to be excited. Silicon wafers develop surface defects during manufacturing and contact, which increases the loss. This limits the Q factor of the silicon disk. For the following tomography study, the disk coating was removed and the geometry of the wafer was partitioned on all edges and faces of the disk, creating a $10\mu m$ shell separating the disk's surface from the bulk silicon. The same SER study has been conducted, comparing the thin surface, around the entire wafer to the loss in the bulk.

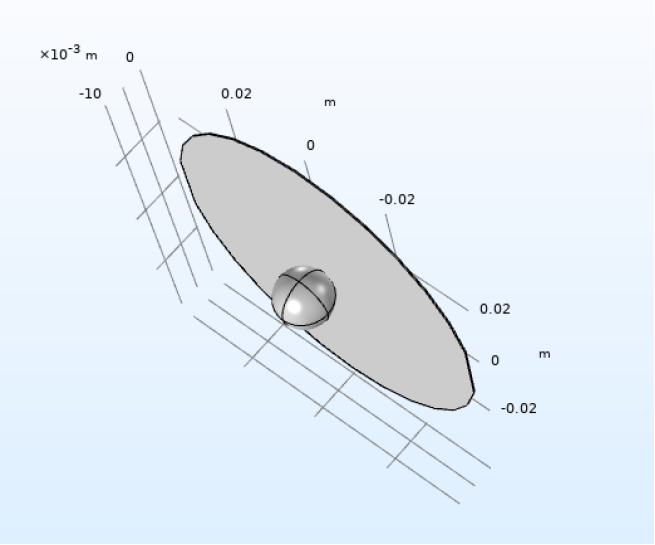

FIG. 6. Geometry of disk model, nodal suspension modelled as point contact between disk and a spherical lens.

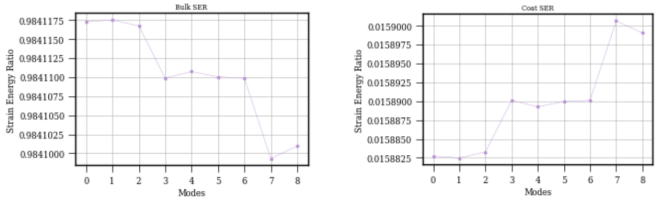

FIG. 7. SER of the bulk of the disk versus the thin film coating (silicon) of the disk for the first 8 modes in COMSOL

III. ANALYSIS AND RESULTS

Combining experimental and modelled results, we were able to solve for unknown losses in our silicon wafer. First, a simple example of the loss tomography method using two known loss angles found experimentally and the COMSOL calculated SER between different disk areas. Using these known parameters we were able to solve for the loss contributions from the surface and the bulk of the wafer (Figure 8).

Now that the final loss angles can be solved for, the next step is adding more parameters and solving for more losses. The next step will be adding a third loss measurement and

$$\begin{pmatrix} SER_{bulk,1} & SER_{surface,1} \\ SER_{bulk,2} & SER_{surface,2} \end{pmatrix}^{-1} \begin{pmatrix} \phi_1 \\ \phi_2 \end{pmatrix} = \begin{pmatrix} \phi_{substrate} \\ \phi_{surface} \end{pmatrix} \quad (6)$$

Q factor	Loss angle	SER_{BULK}	$SER_{SURFACE}$
$5*10^6$	$0.2*10^{-6}$	0.984108	0.015892
$4*10^6$	$0.25*10^{-6}$	0.984117	0.015883

$$\begin{pmatrix} \phi_{sub} \\ \phi_{surf} \end{pmatrix} = \begin{matrix} 1.03 * 10^{-7} \\ 9.79 * 10^{-6} \end{matrix}$$

FIG. 8. Example of the initial 2 by 2 loss tomography matrix calculation. Here we are solving for two unknowns, surface and bulk loss, using experimental and modelled results.

calculating the thermoelastic loss of the disk. With the value known for thermoelastic loss, the temperature of the disk can be known with higher accuracy as well. Then, we will continue the process, solving for more losses. The final step will be minimizing the loss of silicon as much as possible and moving on to measure the losses on thin film coatings on the wafer to identify the best choice for the thin film coatings on the new tests masses in LIGO Voyager.

After the first stage of this analysis is complete, we will use MCMC methods to make these same parameter estimations. With the loss contributions of silicon wafers calculated, the next step will be to minimize these as much as possible. With the silicon losses low and consequentially, the Q-factors very high, thin film coatings on silicon can be investigated. With the confidence the loss measurements of the thin films are significantly greater than those from the silicon, the thin films can be accurately compared. This will allow the thin film coatings in the LIGO Voyager updates to be as low-loss as possible.

ACKNOWLEDGMENTS

We thanks these groups: Bobs, LIGO, Q-factor folk.
Grant number: 12710827401820X.

Appendix A: Appendixes

maybe this is more detail on the MCMC and sensitivity to priors

[1] Brett Shapiro, Rana X Adhikari *Cryogenically cooled ultra low vibration silicon mirrors for gravitational wave observatories*. Cryogenics Volume 81, January 2017, Pages 83-92 (2017)
[2] E. Cesarini, M. Lorenzini *A "gentle" nodal suspension for measurements of the acoustic attenuation in materials*. Rev. Sci. Instrum. 80, 053904 (2009)
[3] J. P. Zendri, M. Bignotto *Loss budget of a setup for measuring mechanical dissipations of silicon wafers between 300 and 4 K*. Review of Scientific Instruments 79, 033901 (2008)
[4] Blevins *Loss budget of a setup for measuring mechanical dissipations of silicon wafers between 300 and 4 K*. Review of Scientific Instruments 79, 033901 (2008)
[5] Virginia Semiconductor Custom 2